Nano Today 39 (2021) 101226

Contents lists available at ScienceDirect

Nano Today

journal homepage: www.elsevier.com/locate/nanotoday

In-situ control of on-chip angstrom gaps, atomic switches, and molecular junctions by light irradiation

Surong Zhang[a], Chenyang Guo[a], Lifa Ni[a], Kerstin M. Hans[b], Weiqiang Zhang[a], Shoujun Peng[a], Zhikai Zhao[a], Daniel C. Guhr[b], Zhe Qi[a], Haitao Liu[a], Minwoo Song[d], Qingling Wang[a], Johannes Boneberg[b], Xuefeng Guo[c,*], Takhee Lee[d,*], Elke Scheer[b,*], Dong Xiang[a,*]

[a] *Tianjin Key Laboratory of Micro-scale Optical Information Science and Technology, Institute of Modern Optics and Center of Single Molecule Sciences, College of Electronic Information and Optical Engineering, Nankai University, 300350 Tianjin, China*
[b] *Department of Physics, University of Konstanz, D-78457 Konstanz, Germany*
[c] *Beijing National Laboratory for Molecular Sciences, State Key Laboratory for Structural Chemistry of Unstable and Stable Species, College of Chemistry and Molecular Engineering, Peking University, Beijing 100871, China*
[d] *Department of Physics and Astronomy, and Institute of Applied Physics, Seoul National University, Seoul 08826, South Korea*

ARTICLE INFO

Article history:
Received 9 March 2021
Received in revised form 19 May 2021
Accepted 14 June 2021
Available online xxxx

Keywords:
Angstrom gaps
Atomic switches
Thermal expansion
Light heating
Break junctions
Single-molecule study

ABSTRACT

Pairs of electrodes with nanometer gap, termed as nano-gapped electrodes, are fundamental building blocks for the fabrication of nanometer-sized devices and are essential for the examination of molecular properties and extreme nano-optics. Although modern fabrication techniques make it feasible to fabricate nanometer gaps, it is still a formidable challenge to fabricate adjustable gaps arrays with angstrom precision. Here, we demonstrate that *in-situ* adjustable nanogaps (arrays) with sub-angstrom precision can be fabricated *via* laser irradiation on the substrate which supports the electrode pairs. We further demonstrate that atomic-level metal contacts can be switched and the direction of the switching can be selectively controlled by the laser irradiation position. By varying the laser power gradually, the nanogap's size can be continuously changed, providing a reliable break junction technique to address the properties of single-molecule junctions. The small spatial focus size of the laser beam makes it feasible to realize addressable on-chip molecular junction arrays.

© 2021 Elsevier Ltd. All rights reserved.

Introduction

Controllable nanogaps with atomic precision are highly desired for the fabrication and characterization of nano-sized devices [1–3], promoting the fast development of extreme nano-optics [4–6]. Modern fabrication techniques, such as standard electron beam lithography (EBL), nanoimprint lithography and crack-defined technique [7,8] make it feasible to fabricate a pair of electrodes (or electrode arrays) with nanometer precision [9–11]. These nanogaps are on-chip compatibility and have been widely used in different research fields. However, these on-chip nanogaps are usually fixed, *i.e.*, the gap cannot be flexibly adjusted after the fabrication process [1,12]. To this end, we demonstrate that precisely adjustable nanogaps with atomic precision could be realized *via* light illumination on the supporting substrate under the electrodes, and various materials (*e.g.*, gold, platinum, aluminum) can be used as electrodes, and common materials (*e.g.*, polyimide, insulation tape) can be used as the supporting substrate.

Besides nano-gapped electrodes, switches are essential elements for electronic circuits [13,14]. Atomic scale switches meet the urgent demand for further device miniaturization and several strategies have been put forward to realize atomic switches [13,15–17]. The realization of light-induced conductance switching has attracted intensive attention recently [18,19]. Several groups had previously demonstrated that single molecule can be used to realize the reversible conductance switching *via* light stimulation [18,20]. Here, we demonstrate that conductance switching also can be realized through light irradiation with bare metal electrodes (without any molecules present). Although the conductance changes of the bare atomic metal contacts depending on the electrodes' geometry, the wavelength, the polarization, and the intensity of the illuminated lasers have been investigated previously, the dominating mechanism for the conductance change is still under debate which had been

* Corresponding authors.
E-mail addresses: guoxf@pku.edu.cn (X. Guo), tlee@snu.ac.kr (T. Lee), elke.scheer@uni-konstanz.de (E. Scheer), xiangdongde@126.com (D. Xiang).

https://doi.org/10.1016/j.nantod.2021.101226
1748-0132/© 2021 Elsevier Ltd. All rights reserved.

attributed to several possible factors including metal electrodes' expansion, plasmonic heating, optical rectification, and photon-assisted transport [3,21–24]. In this work, we clarify with solid evidences that the thermal expansion of the substrate underneath the suspended electrodes should be the main mechanism for the conductance modulation of the suspended atomic contacts. Assisted by simulations, we reveal that the light-induced displacement of the electrodes *via* the thermal expansion of the underneath substrate should be the primary mechanism for the nanogap and atomic contact modulation. Moreover, we demonstrate that the direction of the atomic conductance switching (the conductance increases or decreases upon light irradiation) can be well controlled by adjusting the irradiation position of the focused laser. Finally, we demonstrated that the laser beam (only micrometers in focus diameter) remotely controlled gap size can be used to determine the single-molecule properties (*e.g.*, conductance), showing potential for integrated molecular devices application.

Results

Gap size modulation with sub-angstrom precision by light irradiation

The experiments are performed based on a nanojunction which can be fabricated by different methods [25–28]. Here, the mechanically controllable break junction (MCBJ) is utilized to obtain the initial nanocontacts (Supplementary Fig. S1) [29–32]. Fig. 1(a) shows the working principle of MCBJ. A microwire with a constriction is fixed on the substrate by two drops of glue. The substrate is mounted

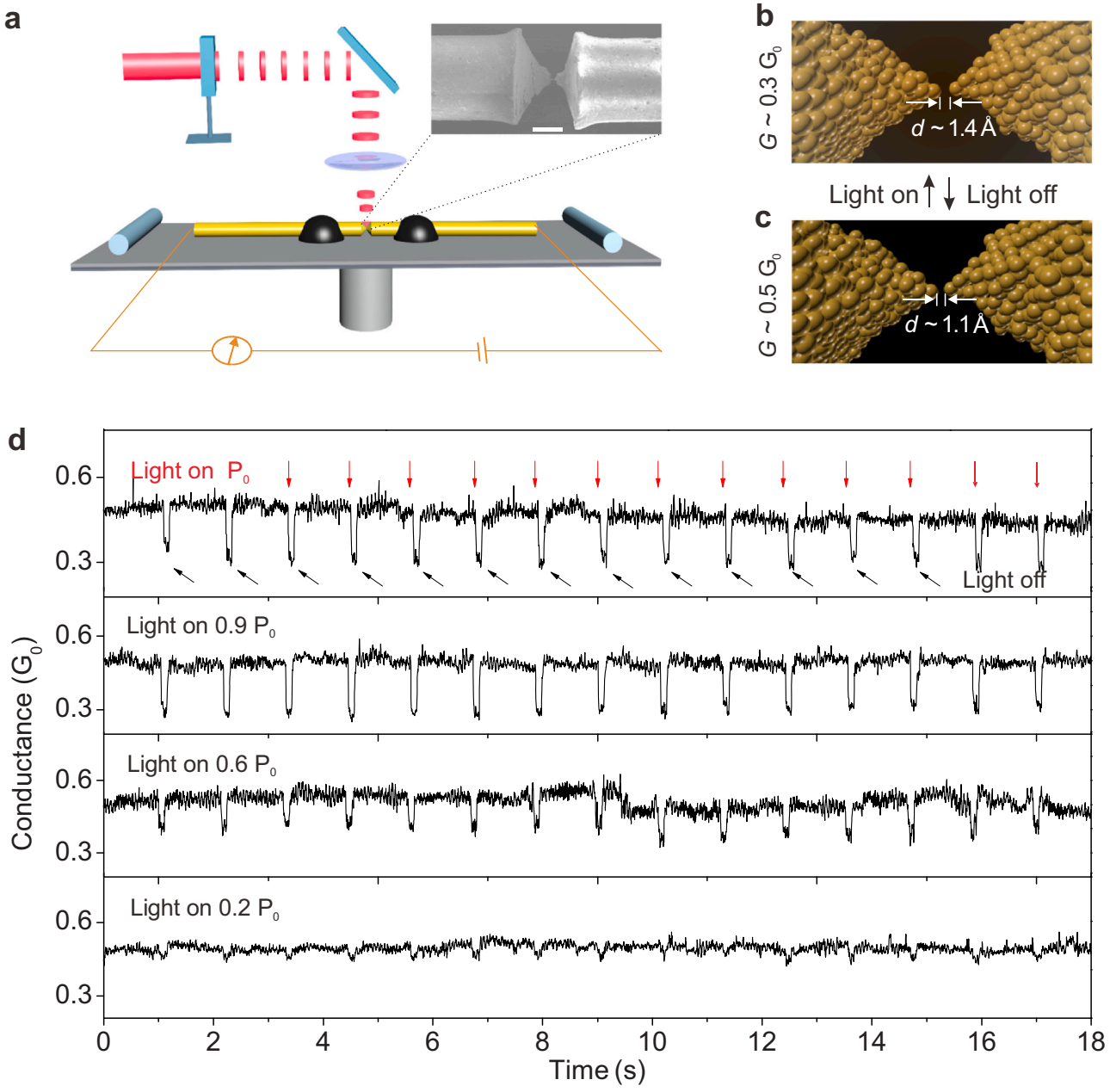

Fig. 1. Schematic of the measurement system and conductance responses of nano-gapped electrodes upon laser irradiation. (a) The continuous laser passes through a chopper generating a periodically pulsed laser beam, then focuses on the wire constriction. Inset: SEM images of the notched microwire. Scale bars: 20 μm. Schematic of the atomic arrangement around the nanogap electrodes with (b) and without (c) laser irradiation. Upon laser irradiation with a power of P_0, the gap size between the two electrodes is enlarged approximately from 1.1 Å to 1.4 Å, as deduced by the measured conductance values. (d) Real-time conductance responses upon laser irradiation with various laser powers. The red (black) arrows indicate the moments when the light is turned on (off). P_0 = 0.4 mW.

into a three-point bending apparatus, in which the two outer posts (blue bars) at either end of the substrate are fixed. The motion of the pushrod (piezo actuated) exerts a vertical bending force onto the substrate, thus the constriction part will be elongated. In this way, a nanocontact between two electrodes can be obtained, *i.e.* a constriction as thin as a single atom but being still an unbroken bridge between both electrodes. Also, a nanogap can be generated by mechanically bending the substrate a bit more and thereby breaking the atomic bridge. To address the sensitivity of the gap size modulation by light irradiation, an extremely small gap (d ~ 1.1 Å) was tested firstly.

Via modulation of a chopper, the continuous laser periodically irradiates (light on for 100 ms and light off for 1 s) the constriction part with a focusing diameter of ~ 0.5 mm. The gap size between electrodes is monitored by the measured tunneling current [33]. Fig. 1(b) and (c) show the schematic of the atomic arrangement around the nanogap electrodes: the gap size between the two electrodes is enlarged approximately from 1.1 Å to 1.4 Å upon light irradiation (P_0 = 0.4 mW). Fig. 1(d) shows that the conductance decreases as the laser irradiates the nanogap area when a fixed bias voltage (13 mV) is applied. In the initial state (in dark), the conductance of the nanogap is approximately 0.5 G_0, which corresponds to a gap size of approximately 1.1 Å (Supplementary Fig. S2). Upon laser irradiation (P_0), the conductance decreases to 0.3 G_0 (gap size ~ 1.4 Å), *i.e.* the gap size is enlarged by ~ 0.3 Å. A close examination of the curves shows that the amplitude of the conductance modulation decreases as the laser power is decreased. Gap size variations of approximately 0.3 Å, 0.2 Å, and 0.1 Å upon laser irradiation with a power of P_0, 0.9 P_0, and 0.6 P_0, respectively, can be deduced, indicating that the gap size can be modulated with sub-atomic precision. Upon even lower irradiation power (P < 0.2 P_0), the conductance response cannot be clearly resolved (bottom curve in Fig. 1d). Notably, with the measured conductance in the range of 0.5 G_0 to 0.3 G_0 the electrodes are very close together. At such small

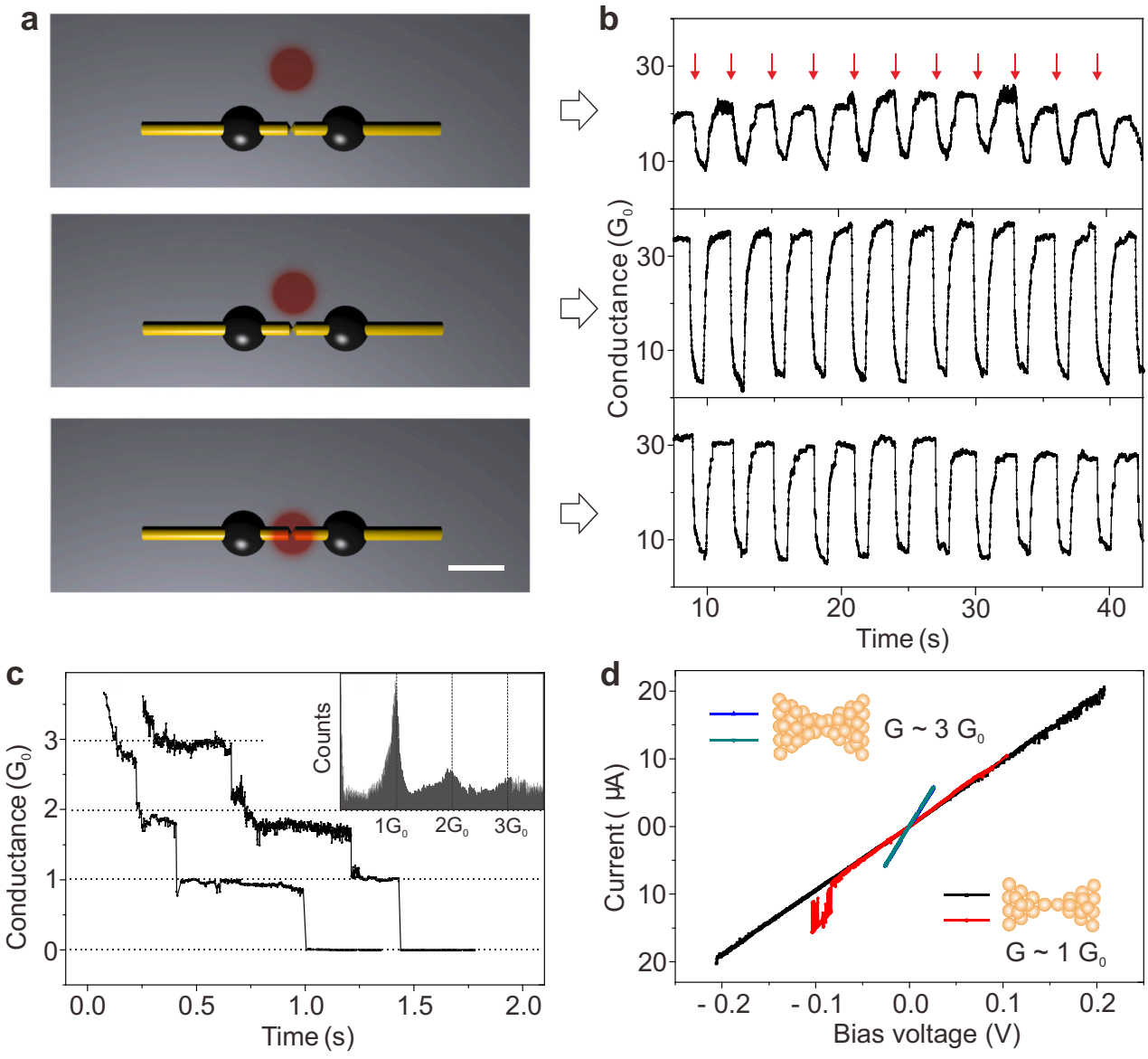

Fig. 2. Conductance response when the laser irradiates aside the nanocontact. (a) Schematics of the situations for laser irradiation in which the laser focal spot are located at the atomic point contact (bottom), 0.5 mm (middle) or 1.5 mm (top) away from the nanocontact. The red area indicates the laser irradiated spot. (b) Real-time measured conductance when the laser irradiates three different spots, as shown in Fig. 2(a). The red arrows indicate the beginning of the light irradiation with a duration of 1 s, followed by a dark time of 2 s (c) Two examples of conductance curves as a function of time under laser irradiation. The conductance decreases in steps of ~ G_0 during the breaking process of the nanocontact. Inset: a corresponding conductance histogram constructed from 500 conductance traces as shown in (c). (d) *I-V* curves of the atomic contacts generated by the control of light irradiation.

distances the front-most atoms may be pulled out of their equilibrium positions by the attractive bonding force, resulting in a poor approximation of the gap size, thus the tunnel approximation is not valid anymore. To remain in the range of validity thereby obtaining a better estimation of the gap size, measurements at larger tunneling distance were also performed (Supplementary Fig. S2).

Modulation of atomic contacts by light-irradiation

In addition to the nanogaps ($G < G_0$), the response of direct electrode nanocontacts ($G > G_0$) to laser irradiation is investigated. The state of the initial nanocontacts is recognized by monitoring the conductance of the junction (a few G_0 to a few tens of G_0). The irradiation sites are selected along the direction perpendicular to the electrode axis, as shown in Fig. 2(a). A similar phenomenon is observed, *i.e.*, the conductance decreases when the nanocontact is irradiated by the laser (bottom panel, Fig. 2b). Notably, the amplitude of the conductance modulation increases as the irradiation spot is moved away from the metal nanocontact, *i.e.,* the amplitude of the conductance modulation increases by approximately 20% as the irradiation spot is moved 0.5 mm away from the center nanocontact (middle panel, Fig. 2b). The amplitude of the conductance modulation decreases when the irradiation spot is moved farther away from the nanocontact area (top panel, Fig. 2b). This observation shows that the conductance of the nanocontact can be strongly modulated even when direct light irradiation to the nanocontact is absent, indicating that the conductance modulation may originate from the properties of the supporting substrate rather than the nanocontact itself. This observation will be further addressed in the discussion part.

Notably, the exact amplitude of the conductance modulation depends on the laser power, focus diameter, the position of the incident laser, and the distance between the two glue drops. Samples with a longer distance between the glue drops show a more sensitive modulation effect. For these samples, the nanocontact may be completely broken upon light irradiation, such that G decreases in discrete steps of the order of G_0, and these discrete steps can be reproducibly observed. Two examples of such conductance curves are shown in Fig. 2(c). The corresponding histogram shows well-defined peaks near $1\,G_0$, $2\,G_0$, and $3\,G_0$ (insert, Fig. 2c). This observation indicates that the geometry of the constriction is changed upon light irradiation [16,34]. With properly chosen light intensity and incident positions, the nanocontacts can be stabilized for several minutes, making it feasible to characterize electron transport through these atomic-size constrictions, down to the single-atom regime. Fig. 2(d) shows several typical current-voltage (I–V) curves within different bias windows for atomic contacts ($1\,G_0$ and $3\,G_0$). Although occasionally switching events (red) and stochastic fluctuations (black) may be observed at high biases, the main linear dependence and thus metallic I–V characteristic are evident. The occasionally switching events at high biases are attributed to the current-induced rearrangement of individual atoms near the constriction [16]. The linear behavior without fluctuations in the small bias range demonstrates that the stability of the atomic contact is retained despite light irradiation.

To reveal the underlying mechanism of the light-induced conductance changes, we performed the conductance measurements with the fixed junction, while the irradiation site moved along the electrode axis. Three different irradiation sites along the metal wire are selected, marked as I, II, and III. Fig. 3(a)–(c) show the situations when the laser irradiates at the left (case I) or right side (case III) of the metal wire, or at the middle constriction part of the wire between two glue drops (case II). Remarkably, the conductance increases upon light irradiation in cases I and III (Fig. 3d and Supplementary Video S1). In contrast, the conductance decreases upon light irradiation in case II (Fig. 3d and Video S2). These

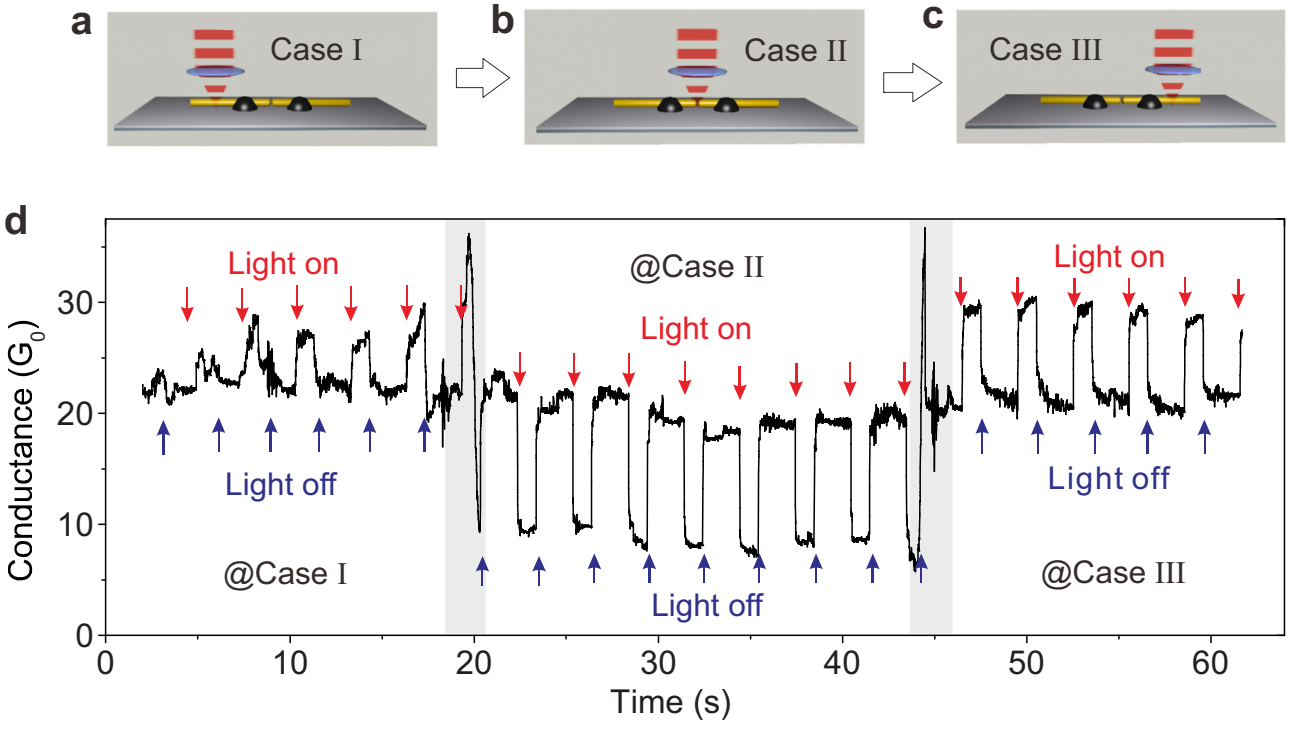

Fig. 3. Real-time conductance measurement of the gold wire when different spots of the wire are irradiated by the laser. The light irradiates the (a) left part of the wire fixed by two drops of glue, (b) the central constriction of the wire, and (c) the light irradiates the right part of the wire. (d) Current response of the gold wire when different parts of the wire (as shown in a, b, and c) are irradiated by the laser. The red arrows indicate the begin of the irradiation by the laser with a duration of 1 s, and the blue arrows indicate that the laser is turned off (3 s for one cycle). The two gray regions indicate the transition regimes in which the irradiation spots are changed (from case I to case II, or from case II to case III).

observations evidence that the sign of the conductance change (increase or decrease upon light irradiation) can be well controlled by selecting an appropriate laser irradiation position.

Supplementary material related to this article can be found online at doi:10.1016/j.nantod.2021.101226.

We further performed a similar experiment in which the light irradiates the supporting substrate instead of the metal wire, and the irradiated sites are selected along the direction parallel to the electrode axis. Again, we observe that the conductance decreases upon laser irradiation when the light illuminates inside the region defined by the two glue drops (Supplementary Fig. S3). In contrast, the conductance increases when irradiating outside the region defined by the two glue drops. Based on the observations mentioned above, we believe that the conductance modulation should originate mainly from the thermal expansion of the underneath polymer substrate, *i.e.*, the light-induced thermal expansion of the substrate will lead to a relative position change of the two electrodes which are fixed above the substrate, thus resulting in conductance modulation, which will be further addressed in more detail in the simulation part.

Additionally, our experiments show that the temperature increase of the irradiated area is relatively small under laser irradiation (Supporting Fig. S4). Various materials (*e.g.*, Au, Pt, and Al) can be used as working electrodes (Supplementary Fig. S5), and universal materials (*e.g.*, polyimide, Kapton tape, and even bare spring steel) can be used as the supporting substrate (Supplementary Fig. S6). Importantly, we demonstrate that the conductance modulation of parallel junctions can be operated independently (Supplementary Fig. S7), providing potential for device integration. All these features might make the light-control strategy a versatile approach for the conductance modulation.

Simulation of light-induced thermal expansion

To verify that the gap size control, as well as the bidirectional atomic contact modulations, originate mainly from thermal expansion of the supporting substrate, we performed thermal expansion simulations of the polymer substrate with the software package COMSOL Multiphysics. Fig. 4(a) and (b) show the distribution of thermal expansion of the polymer substrate with different thickness. The expansion is directed outwards from the irradiation point. It can be found that the amplitude of the thermal expansion is strongly dependent on the thickness of the polymer substrate for the same laser focus diameter (0.5 mm), *i.e.*, the maximum thermal expansion increases from 0.04 Å to 24 Å when the thickness of the polymer layer increases from 5 µm to 150 µm. The maximum expansion reaches 12 Å as a polymer layer (50 µm thickness) is employed (Supplementary Fig. S8), which is consistent with experimentally measured thermal expansion coefficients of polymer [35], confirming the reliability of the simulations. The thermal expansion

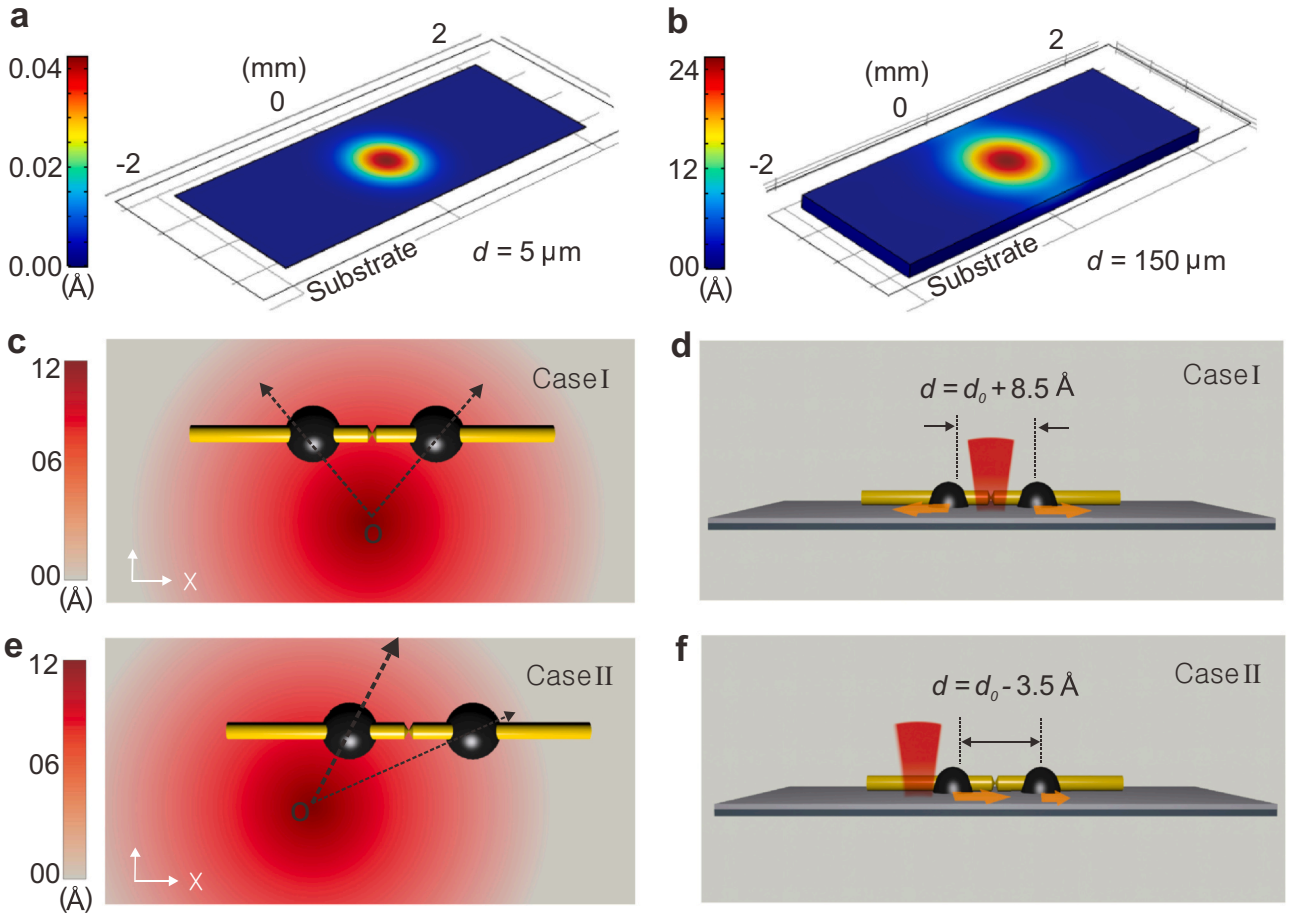

Fig. 4. Simulation of thermal expansion and mechanism analysis for the bidirectional gap size modulation. Thermal expansion of the polyimide substrate with a thickness of 5 µm (a) and 150 µm (b) upon laser irradiation. "O" indicates the center position of the incident laser. (c) False-color plot of the amplitude of the thermal expansion of the polymer (50 µm in thickness) when the light irradiates an area between the two glue drops. The black arrows indicate the moving direction of the glue drops. (d) Side view of the movement of the two electrodes for the irradiation shown in (c). The orange arrows indicate the moving directions of the two glue drops. The nanocontact will be stretched due to the opposite movement of the two glue drops. (e) Thermal expansion of the substrate when the laser irradiates an area outside the two glue drops. The thickness of the black arrows is positively proportional to the amplitude of the glue's displacement. (f) Side view of the situation as shown in (e). The nanocontact will be compressed due to the unidirectional but unequal movement of the two glue drops upon light irradiation.

around the metal wire is inhomogeneous, which will result in a relative displacement of the two electrodes fixed on the substrate. Fig. 4(c) and (d) show that, for the geometry considered here, the expansion of the polymer layer pushes the two electrodes apart by approximately 8.5 Å, when the laser irradiates the central region. In contrast, the expansion of the polymer layer brings the two electrodes closer together by 3.5 Å as the laser irradiates a site outside the two gluing points, since the two glue drops move in the same direction (X) but with unequal displacement, see Fig. 4(e) and (f). In the simulations, we neglect the presence of the thin steel sheet underneath the polymer layer because the polyimide layer is relatively thick and almost 100% of the light gets absorbed within this thickness (50 µm of polyimide are optically opaque). Regarding the simulation, more detailed information can be found in Supplementary Figs. S8 and S9.

Conductance modulation with minimized junctions

Aiming for device integration, miniaturized junctions (fabricated by electron-beam lithography, EBL) with reduced laser focal spots are investigated. Similar to the results presented in Fig. 3, the conductance decreases as the light irradiates the central constriction of the wire, and the conductance increase as the light irradiates the left/right side of the suspended wire, as shown in Fig. 5(a). A Kapton sheet covered with a thin polyimide layer (1 µm) is used as the substrate. The thickness of the gold layer is approximately 100 nm. The length of the suspended metal bridge is approximately 2 µm, and the width of the constriction center is approximately 100 nm, as presented in Fig. 5(b). The polarization of the laser is along the electron transport direction (wavelength $\lambda = 488$ nm, laser power $P = 126$ µW).

The observation of conductance increases and decreases depending on the position of irradiation reveals the complexity of the mechanism at play. We argue that in the present realization, both effects are caused by thermal expansion. When irradiating the central part with the narrow bridge, the largest part of the spot is absorbed by the underneath substrate which then elongates and thereby reduces the conductance. When irradiating electrodes not too far away from the constriction (~ 20 µm) the thermal expansion of the gold electrodes dominates and therefore the conductance increases. When irradiating the electrodes but at larger distance the influence of the irradiation is vanishing, from which an effective range of the modulation concept by irradiation can be estimated.

Notably, the effect of conductance modulation with this EBL fabricated samples is much weaker than the one of samples made from a wire glued onto the substrate. We attribute this observation to the fact that the distance between two fixed points of the electrodes in EBL fabricated sample is much shorter than the one in glue-fixed samples. The absolute elongation due to thermal expansion is in roughly proportional to the size of the heated area. Hence, the relative displacement of the two electrodes correlates with the distance between the two fixed points of the electrodes. As shown in Fig. 5(b), the length of the suspended gold bridge in EBL fabricated samples is approximately 2 µm, which means the distance between two fixed points of the electrodes is 2 µm. In contrast, the distance between the glue drops in the wire-based break junctions is approximately 0.5 mm, as shown in Fig. 1(a). Therefore, the amplitude of conductance modulation with this EBL fabricated samples is much weaker than the one of glue fixed samples. We can further draw the conclusion that the gap size variation due to substrate expansion can be ignored when the two electrodes are completely fixed on the substrate without free-standing parts and are located close enough (*e.g*, few nanometers separation), because the displacements of such close electrodes upon laser irradiation are synchronous both in direction and amplitude, and thus the relative displacement of the two electrodes is extremely tiny (*e.g*, few picometers). Additionally, we found that the conductance modulation with minimized junctions made by EBL is also dependent on the materials of employed substrates, see Supplementary Figs. S10 and S11 for more detailed information. These miniaturized junctions controlled by focused laser provide a potential for producing individually addressable arrays of molecule junctions.

Determining the conductance of single molecule

Taking advantage of the capability of modulating the electrode separation precisely with the help of laser irradiation, we measured the conductance of single-molecule junctions of *p*-phenylenediamine (PPDA) molecules. To avoid thermal voltages caused by direct laser illumination, the laser illuminates an area perpendicular to the electrode axis approximately 5 millimeters away from the metal wire. As shown in Fig. 6(a), the gold atomic junction is stretched as

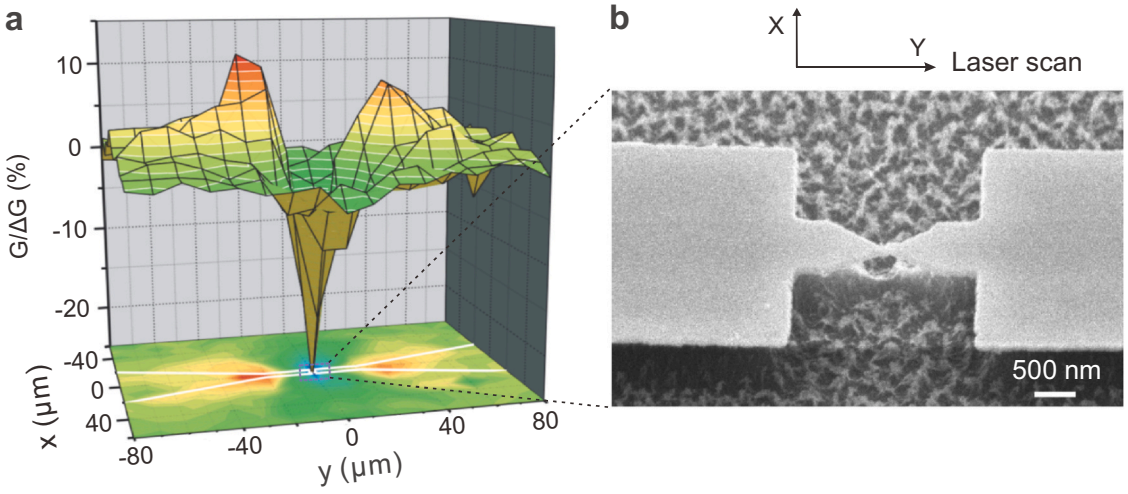

Fig. 5. Conductance-change maps of Au atomic contacts made from lithographic break junctions under light irradiation in vacuum. (a) 3D plots and projected color maps show the relative conductance changes as a function of the position of the laser irradiation. The white lines show the contour of the Au electrodes. The area $-40\,\mu m < x < 40\,\mu m$ and $-80\,\mu m < y < 80\,\mu m$ is scanned. The average conductance of the nanocontact is approximately $6.0\,G_0$. The maximum positive conductance change is $\Delta G/G_{max} = 12\%$, and the maximum negative conductance change is $\Delta G/G_{min} = -26\%$. The focal spot size of the laser is approximately 18 µm. (b) SEM image of the chip under test fabricated by EBL technique.

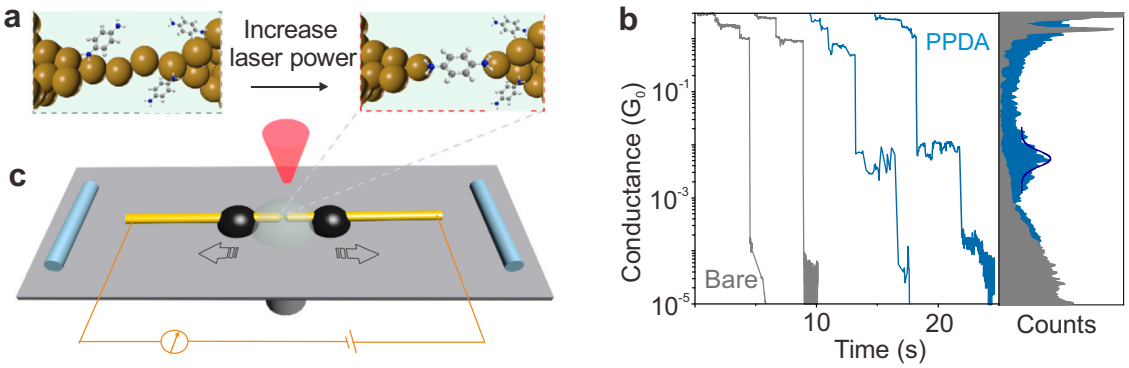

Fig. 6. Measurement of the molecular conductance of PPDA single-molecule junctions by regulating the laser power gradually. (a) Schematic of molecular conductance measurement. The laser illuminates a region aside of the metal junction at a few millimeters distance. The molecular junction is formed during the separation processes of electrodes with an increase of the laser power gradually. The metal junction is surrounded by a drop of 1 mM aqueous solution of PPDA, and a bias voltage of 18 mV is applied to the pair of electrodes. (b) The conductance curves recorded during the electrodes' separation process and corresponding conductance histogram with and without PPDA molecules. The gray curves and histogram are obtained by employing a pure aqueous solution, and the blue one is generated by employing a PPDA containing aqueous solution. Each histogram is constructed by approximately 500 conductance curves. The conductance histogram with molecules shows a peak around 4.3×10^{-3} G_0. The dark blue line represents the Gaussian fit. In contrast, no apparent peak below 1 G_0 is observed for the measurement in the molecule-free solution.

the laser power gradually increases. As a reversible process, a metal contact can be reformed when the laser power gradually decreases. A fiber laser (LWRL635-100mW-F) with a wavelength of 635 nm and adjustable power of 0–30 mW is used as the gap size controller. To form single-molecule junctions, a 1 mM aqueous solution of PPDA is self-assembled on the metal electrodes surface for about 30 min right after the breaking of the metal wire followed by the conductance measurement. Typically, multiple steps of G_0 can be clearly observed in solution both with and without molecule, as shown in Fig. 6(b). For the solution with molecules, additional plateaus are frequently observed after the breaking of metal wire, see blue curves. In contrast, plateaus below 1 G_0 are rarely observed when the sample is measured in an environment without PPDA molecules, see gray curves.

Fig. 6(b) shows the conductance histograms for both with and without PPDA molecules, and each of them is constructed from approximately 500 conductance curves. With a Gaussian fit, the most-probable conductance value (~ 4.3×10^{-3} G_0) at the bias of 18 mV can be determined for the solution containing molecules. In contrast, no obvious peak is observed in the histogram after break of the metal wire for a solution without molecules. Therefore, the conductance value (~ 4.3×10^{-3} G_0), which is consistent with previous reports [36,37], can be assigned to the conductance of a single PPDA molecule junction. Similar to the atomic contacts presented in Fig. 2(d), the single-molecule junctions can be sustained for several minutes under a constant laser power, and thus the *I–V* characteristics of single-molecule junctions can be addressed.

Discussion

Returning to Fig. 2, it shows an interesting phenomenon, *i.e.*, the maximum conductance modulation appears when the laser is focused aside of the nanocontact instead of onto the nanocontact directly. This observation is consistent with our previous report that the metal nanocontact itself expands upon laser illumination [22,38], which brings the two electrodes closer together, and thus partially compensates the expansion of the underneath polymer substrate which separates the two electrodes. Our previous study revealed *via* wavelength and polarization-dependent measurements that the thermal expansion of electrodes is considerable (up to nanometers) due to plasmonic heating [22]. The expansion of the electrodes will result in a weaker conductance modulation by the thermal expansion of the supporting substrate. Additionally, the plasmon excitation and photon-assisted electron transport between electrodes may increase the conductance [21,39–41], which will also weaken the modulation effect by the thermal expansion of the supporting substrate.

The modulation of the tunneling current in nanogaps is of key importance for designing opto-nanoelectronic devices. The pioneering research works mainly focus on the photon (plasmon) assisted tunneling between electrodes and the thermal expansion of the electrodes themselves [21,23,38–40,42–44]. In contrast, we focus here on the effect of the substrate's thermal expansion gradients under the electrodes which is usually ignored. Contrary to the geometries in scanning tunneling microscopy (STM) where the STM tip is separated from another electrode (substrate), the pair of electrodes is fixed on the same substrate in our case which is of key importance to control the gap size with angstrom precision. Although the maximum thermal expansion of the substrate driven by the light irradiation is at the nanometer scale, the relative displacement of two close points on the substrate can be reduced to (sub) angstrom, resulting in a precise control of the gap size. Despite this advantage of precise control of our strategy, the initialization of the nanocontacts by bending the substrate in our experiment is essential for breaking the metal wire by light irradiation, which may limit its practical application. Note that these initial nanocontacts can also be generated by other chip compatible approaches without substrate bending, *e.g.*, electrochemical deposition or electromigration.

Thermal expansion had been considered as a failure mode since it unintentionally changes the shape of the object evidently. Correspondingly, the thermal expansion of substrate was never pursued as a concept for the fabrication of nano/molecule junctions. Normally, to *in-situ* control the nanogaps and form single-molecule junctions, an electric piezo/motor actuator (decimeters/centimeters in spatial size) is required [45]. Each piezo/motor element can only control one nanogap normally, which makes it challenging to fabricate wafer-scale compatible integrated molecular junction arrays [17]. Here, we demonstrated that a focused laser beam (only micrometers in diameter) can work as an actuator to remotely control the gap size to form single-molecule junctions repeatedly, in principle for thousands of times in parallel, making it feasible to produce individually addressable arrays of molecular junctions.

Conclusions

We demonstrate that conductance switching can be realized through light irradiation with bare electrodes, and the switch

direction can be well controlled by adjusting the incident position of the light. In this way, triple states conductance switches are realized *via* laser irradiation. Supported by simulations, we clarify that the atomic switch, as well as the gap size modulation, originate mainly from the thermal expansion gradients of the underneath substrate upon light irradiations. We further demonstrate that the nanogap between two electrodes can be gradually modulated with sub-angstrom precision by the control of the laser power, providing a light remotely controlled on-chip break junction technique for the study of single-molecule junctions. The small focus diameter of laser beams making it feasible to realize an addressable molecule junction array.

Methods

Sample preparation

Elastic steel sheets (length of 44 mm, width of 12 mm, and thickness of 0.2 mm) are used as flexible bending substrates, on which a polymer layer (polyimide, HD-4100, HD Microsystem, ~ 50 µm thick) is spin-coated. The substrate is baked in an oven at 200 °C for half hour to harden the polyimide. A gold wire (100 µm, 99.999%) is then fixed on the polyimide covered spring steel substrate by two drops of glue (epoxy resin, STYCAST 2850 FT). To facilitate the breaking of the metal wire, a round notch is made by a surgical knife [22,29].

Conductance measurement and laser irradiation

A voltage (13 mV) is applied to the two electrodes, and the real-time current response upon light irradiation is recorded in ambient by a semiconductor device analyzer (B1500A, KEYSIGHT). To measure the conductance, an ASU (atto sense/switch unit) and integrated amplifiers are added to promote the measurement sensitivity. A He-Ne laser (633 nm, 0.4 mW) is used as the light source. Reflected by a mirror, the laser passes through two polarizers and then focuses on the sample surface (diameter of the spot ~ 0.5 mm). The position of the laser irradiation spots can be precisely changed *via* the mirror as well as by the movement of the platform in two orthogonal directions. The intensity of the laser can be modulated by changing the relative angle of two polarizers. Additionally, an argon-krypton laser is used as the light source, which allows us to select one of several wavelengths in the range between 480 nm and 650 nm with focus diameter 18 µm for EBL microfabricated chips.

Simulation of thermal expansion

To study the distribution of the thermal expansion of the polymer upon light irradiation, two coupled modules including the "heat transfer in solids" and "solid mechanics" modules of the COMSOL Multiphysics software are used. The thermal expansion coefficient of the polymer is set to 2×10^{-5} K^{-1}, the Young's modulus is set to 2.9 GPa, and the Poisson's ratio is set to 0.41. The heat capacitance of polyimide is set to 1100 J kg^{-1} K^{-1}, and the thermal conductance is set to 0.15 WK^{-1} m^{-1}, as report previously [42]. The polymer is irradiated with a Gaussian-shaped heat source (0.5 mm in diameter, and 0.4 mW in power). The initial temperature of the polymer is set to 296 K, which is close to the ambient experimental conditions. Perfectly Matched Layer (PML) is chosen as the boundary condition, which applies to all exterior boundaries.

Funding

This work was supported by the National Natural Science Foundation of China (91950116, 11804170); Natural Science Foundation of Tianjin (19JCZDJC31000, 19JCJQJC60900); the National Research Foundation grant (No. 2021R1A2C3004783) by the Ministry of Science and ICT of Korea; German Research Foundation (Deutsche Forschungsgemeinschaft–DFG) through SFB 513 and 767 and the Strategic Japanese-German Cooperative Program of the JST and DFG on Nanoelectronics; the Ministry of Science and Arts Baden-Württemberg through the Center of Applied Photonics and the Baden-Württemberg Foundation in the framework of the Research Network Functional Nanostructures.

CRediT authorship contribution statement

Takhee Lee, Elke Scheer, Xuefeng Guo, and Dong Xiang initiated the project. Surong Zhang, Kerstin M. Hans, Weiqiang Zhang, Elke Scheer and Dong Xiang designed the experiments. Surong Zhang, Chenyang Guo, Shoujun Peng, Kerstin M. Hans and Daniel C. Guhr fabricated the samples and performed the electrical measurement. Surong Zhang and Zhikai Zhao did the simulations. Surong Zhang and Lifa Ni measured the temperature. Surong Zhang, Qingling Wang and Zhikai Zhao characterized the samples. Surong Zhang, Elke Scheer, Takhee Lee, Haitao Liu, Minwoo Song and Dong Xiang analyzed the data. Surong Zhang and Xuefeng Guo wrote the manuscript with contributions from the other authors.

Declaration of Competing Interest

The authors declare that they have no known competing financial interests or personal relationships that could have appeared to influence the work reported in this paper.

Acknowledgements

We thank Prof. F. Stoddart, Dr. D. Mayer, Prof. P. Leiderer, Prof. J. C. Cuevas, Prof. D. G. Cahill, Dr. R. Waitz and Dr. T. B. Möller for fruitful discussions, and L. Kukk and A. Fischer for the technical assistance.

Appendix A. Supporting information

Supplementary data associated with this article can be found in the online version at doi:10.1016/j.nantod.2021.101226.

References

[1] T. Li, W. Hu, D. Zhu, Nanogap electrodes, Adv. Mater. 22 (2010) 286–300.
[2] J. Xiang, B. Liu, S.-T. Wu, B. Ren, F.Z. Yang, B.W. Mao, Y.L. Chow, Z.Q. Tian, A controllable electrochemical fabrication of metallic electrodes with a nanometer/angstrom-sized gap using an electric double layer as feedback, Angew. Chem. Int. Ed. Engl. 44 (2005) 1265–1268.
[3] D.R. Ward, F. Hüser, F. Pauly, J.C. Cuevas, D. Natelson, Optical rectification and field enhancement in a plasmonic nanogap, Nat. Nanotechnol. 5 (2010) 732–736.
[4] J.J. Baumberg, J. Aizpurua, M.H. Mikkelsen, D.R. Smith, Extreme nanophotonics from ultrathin metallic gaps, Nat. Mater. 18 (2019) 668–678.
[5] F. Benz, M.K. Schmidt, A. Dreismann, R. Chikkaraddy, Y. Zhang, A. Demetriadou, C. Carnegie, H. Ohadi, B. de Nijs, R. Esteban, J. Aizpurua, J.J. Baumberg, Single-molecule optomechanics in “picocavities”, Science 354 (2016) 726–729.
[6] Y.M. Bahk, D.S. Kim, H.R. Park, Large-area metal gaps and their optical applications, Adv. Opt. Mater. 7 (2019) 1800426.
[7] V. Dubois, F. Niklaus, G. Stemme, Crack-defined electronic nanogaps, Adv. Mater. 28 (2016) 2178–2182.
[8] V. Dubois, F. Niklaus, G. Stemme, Design and fabrication of crack-junctions, Microsyst. Nanoeng. 3 (2017) 17042.
[9] P. Gu, W. Zhang, G. Zhang, Plasmonic nanogaps: from fabrications to optical applications, Adv. Mater. Interfaces 5 (2018) 1800648.
[10] Y.Y. Choi, T. Teranishi, Y. Majima, Robust Pt-based nanogap electrodes with 10 nm scale ultrafine linewidth, Appl. Phys. Express 12 (2019) 025002.

[11] M. Zhang, Q. Deng, L. Shi, A. Cao, H. Pang, S. Hu, Nanobowl array fabrication based on nanoimprint lithography, Optik 127 (2016) 145–147.
[12] D. Xiang, X. Wang, C. Jia, T. Lee, X. Guo, Molecular-scale electronics: from concept to function, Chem. Rev. 116 (2016) 4318–4440.
[13] K. Terabe, T. Hasegawa, T. Nakayama, M. Aono, Quantized conductance atomic switch, Nature 433 (2005) 47–50.
[14] C. Arima, A. Suzuki, A. Kassai, T. Tsuruoka, T. Hasegawa, Development of a molecular gap-type atomic switch and its stochastic operation, J. Appl. Phys. 124 (2018) 152114.
[15] F.Q. Xie, X.H. Lin, A. Gross, F. Evers, F. Pauly, T. Schimmel, Multiplicity of atomic reconfigurations in an electrochemical Pb single-atom transistor, Phys. Rev. B 95 (2017) 195415.
[16] C. Schirm, M. Matt, F. Pauly, J.C. Cuevas, P. Nielaba, E. Scheer, A current-driven single-atom memory, Nat. Nanotechnol. 8 (2013) 645–648.
[17] F. Evers, R. Korytár, S. Tewari, J.Mv Ruitenbeek, Advances and challenges in single-molecule electron transport, Rev. Mod. Phys. 92 (2020) 035001.
[18] C. Jia, A. Migliore, N. Xin, S. Huang, J. Wang, Q. Yang, S. Wang, H. Chen, D. Wang, B. Feng, Z. Liu, G. Zhang, D.-H. Qu, H. Tian, M.A. Ratner, H.Q. Xu, A. Nitzan, X. Guo, Covalently bonded single-molecule junctions with stable and reversible photoswitched conductivity, Science 352 (2016) 1443–1445.
[19] D. Dulic, S.J. van der Molen, T. Kudernac, H.T. Jonkman, J.J.D. de Jong, T.N. Bowden, J. van Esch, B.L. Feringa, B.J. van Wees, One-way optoelectronic switching of photochromic molecules on gold, Phys. Rev. Lett. 91 (2003) 207402.
[20] N. Darwish, A.C. Aragonès, T. Darwish, S. Ciampi, I. Díez-Pérez, Multi-responsive photo- and chemo-electrical single-molecule switches, Nano Lett. 14 (2014) 7064–7070.
[21] D.C. Guhr, D. Rettinger, J. Boneberg, A. Erbe, P. Leiderer, E. Scheer, Influence of laser light on electronic transport through atomic-size contacts, Phys. Rev. Lett. 99 (2007) 086801.
[22] W. Zhang, H. Liu, J. Lu, L. Ni, H. Liu, Q. Li, M. Qiu, B. Xu, T. Lee, Z. Zhao, X. Wang, M. Wang, T. Wang, A. Offenhaeusser, D. Mayer, W.-T. Hwang, D. Xiang, Atomic switches of metallic point contacts by plasmonic heating, Light Sci. Appl. 8 (2019) 34.
[23] C.I. Evans, P. Zolotavin, A. Alabastri, J. Yang, P. Nordlander, D. Natelson, Quantifying remote heating from propagating surface plasmon polaritons, Nano Lett. 17 (2017) 5646–5652.
[24] N. Ittah, Y. Selzer, Electrical detection of surface plasmon polaritons by 1G0 gold quantum point contacts, Nano Lett. 11 (2011) 529–534.
[25] A.P. Bonifas, R.L. McCreery, 'Soft' Au, Pt and Cu contacts for molecular junctions through surface-diffusion-mediated deposition, Nat. Nanotechnol. 5 (2010) 612–617.
[26] B. Liu, J. Xiang, J.H. Tian, C. Zhong, B.W. Mao, F.Z. Yang, Z.B. Chen, S.T. Wu, Z.Q. Tian, Controllable nanogap fabrication on microchip by chronopotentiometry, Electrochim. Acta 50 (2005) 3041–3047.
[27] D.E. Johnston, D.R. Strachan, A.T.C. Johnson, Parallel fabrication of nanogap electrodes, Nano Lett. 7 (2007) 2774–2777.
[28] Z.M. Wu, M. Steinacher, R. Huber, M. Calame, S.J. van der Molen, C. Schoenenberger, Feedback controlled electromigration in four-terminal nanojunctions, Appl. Phys. Lett. 91 (2007) 053118.
[29] Q. Wang, R. Liu, D. Xiang, M. Sun, Z. Zhao, L. Sun, T. Mei, P. Wu, H. Liu, X. Guo, Z.-L. Li, T. Lee, Single-atom switches and single-atom gaps using stretched metal nanowires, ACS Nano 10 (2016) 9695–9702.
[30] R. Fukuzumi, S. Kaneko, S. Fujii, T. Nishino, M. Kiguchi, Structure and electron transport at metal atomic junctions doped with dichloroethylene, ChemPhysChem 21 (2020) 175–180.
[31] D. Dulić, A. Rates, E. Castro, J. Labra-Munoz, D. Aravena, A. Etcheverry-Berrios, D. Riba-Lopez, E. Ruiz, N. Aliaga-Alcalde, M. Soler, L. Echegoyen, H.S.J. van der Zant, Single-molecule transport of fullerene-based curcuminoids, J. Phys. Chem. C 124 (2020) 2698–2704.
[32] C.J. Muller, J.M. van Ruitenbeek, L.J. de Jongh, Conductance and supercurrent discontinuities in atomic-scale metallic constrictions of variable width, Phys. Rev. Lett. 69 (1992) 140–143.
[33] L. Grüter, M.T. González, R. Huber, M. Calame, C. Schönenberger, Electrical conductance of atomic contacts in liquid environments, Small 1 (2005) 1067–1070.
[34] N. Agraït, A.L. Yeyati, J.M. van Ruitenbeek, Quantum properties of atomic-sized conductors, Phys. Rep. 377 (2003) 81–279.
[35] P. Bing, X. Huimin, H. Tao, A. Asundi, Measurement of coefficient of thermal expansion of films using digital image correlation method, Polym. Test. 28 (2009) 75–83.
[36] J. Tobita, Y. Kato, M. Fujihira, Single molecular conductance measurements of molecular junction of Au/1,4-phenylenediamine/Au, Ultramicroscopy 108 (2008) 1040–1044.
[37] R.M. Metzger, Unimolecular electronics, Chem. Rev. 115 (2015) 5056–5115.
[38] J. Boneberg, H.J. Münzer, M. Tresp, M. Ochmann, P. Leiderer, The mechanism of nanostructuring upon nanosecond laser irradiation of a STM tip, Appl. Phys. A: Mater. Sci. Process. 67 (1998) 381–384.
[39] C.I. Evans, D. Natelson, Remote excitation of hot electrons via propagating surface plasmons, J. Phys. Chem. C 123 (2019) 10057–10064.
[40] N. Ittah, G. Noy, I. Yutsis, Y. Selzer, Measurement of electronic transport through 1G0 gold contacts under laser irradiation, Nano Lett. 9 (2009) 1615–1620.
[41] E.D. Fung, O. Adak, G. Lovatt, D. Scarabelli, L. Venkataraman, Too hot for photon-assisted transport: hot-electrons dominate conductance enhancement in illuminated single-molecule junctions, Nano Lett. 17 (2017) 1255–1261.
[42] D. Benner, J. Boneberg, P. Nuernberger, R. Waitz, P. Leiderer, E. Scheer, Lateral and temporal dependence of the transport through an atomic gold contact under light irradiation: signature of propagating surface plasmon polaritons, Nano Lett. 14 (2014) 5218–5223.
[43] S. Grafström, P. Schuller, J. Kowalski, R. Newmann, Thermal expansion of scanning tunneling microscopy tips under laser illumination, J. Appl. Phys. 83 (1998) 3453–3460.
[44] R. Huber, M. Koch, J. Feldmann, Laser-induced thermal expansion of a scanning tunneling microscope tip measured with an atomic force microscope cantilever, Appl. Phys. Lett. 73 (1998) 2521–2523.
[45] C. Zhan, G. Wang, J. Yi, J.Y. Wei, Z. Li, Z. Chen, J. Shi, Y. Yang, W. Hong, Z.Q. Tian, Single-molecule plasmonic optical trapping, Matter 3 (2020) 1350–1360.